Atmospheric Environment 79 (2013) 787–801

Contents lists available at ScienceDirect

Atmospheric Environment

journal homepage: www.elsevier.com/locate/atmosenv

Implications of alternative assumptions regarding future air pollution control in scenarios similar to the Representative Concentration Pathways

Clifford Chuwah [a,b,c,*], Twan van Noije [a], Detlef P. van Vuuren [b,d], Wilco Hazeleger [a,c], Achim Strunk [a], Sebastiaan Deetman [b], Angelica Mendoza Beltran [b], Jasper van Vliet [b]

[a] Royal Netherlands Meteorological Institute, De Bilt, Netherlands
[b] Netherlands Environmental Assessment Agency, Bilthoven, Netherlands
[c] Wageningen University, Wageningen, Netherlands
[d] Utrecht University, Department of Geosciences, Utrecht, Netherlands

HIGHLIGHTS

- We have developed high and low air pollution emission scenario variants of the RCPs.
- Both climate and air pollution policies are important for future air quality.
- Pollution control can reduce the O_3 and aerosol direct RF under climate mitigation.

ARTICLE INFO

Article history:
Received 23 November 2012
Received in revised form
2 July 2013
Accepted 4 July 2013

Keywords:
Emission scenarios
Representative Concentration Pathways
Climate change mitigation
Air pollution control
Radiative forcing

ABSTRACT

The uncertain, future development of emissions of short-lived trace gases and aerosols forms a key factor for future air quality and climate forcing. The Representative Concentration Pathways (RCPs) only explore part of this range as they all assume that worldwide ambitious air pollution control policies will be implemented. In this study, we explore how different assumptions on future air pollution policy and climate policy lead to different concentrations of air pollutants for a set of RCP-like scenarios developed using the IMAGE model. These scenarios combine low and high air pollution variants of the scenarios with radiative forcing targets in 2100 of 2.6 W m^{-2} and 6.0 W m^{-2}. Simulations using the global atmospheric chemistry and transport model TM5 for the present-day climate show that both climate mitigation and air pollution control policies have large-scale effects on pollutant concentrations, often of similar magnitude. If no further air pollution policies would be implemented, pollution levels could be considerably higher than in the RCPs, especially in Asia. Air pollution control measures could significantly reduce the warming by tropospheric ozone and black carbon and the cooling by sulphate by 2020, and in the longer term contribute to enhanced warming by methane. These effects tend to cancel each other on a global scale. According to our estimates the effect of the worldwide implementation of air pollution control measures on the total global mean direct radiative forcing in 2050 is +0.09 W m^{-2} in the 6.0 W m^{-2} scenario and −0.16 W m^{-2} in the 2.6 W m^{-2} scenario.

1. Introduction

Recently, the research community has developed a set of scenarios (Representative Concentration Pathways, RCPs) to improve understanding of the complex linkages between human activities and the climate system (Moss et al., 2010; Van Vuuren et al., 2011a). These scenarios form the basis of the current generation of climate model runs as part of the Atmospheric Chemistry and Climate Model Intercomparison Project (ACCMIP, Lamarque et al., 2013) and Coupled Model Intercomparison Project (CMIP5, Taylor et al., 2012), which will be used in the fifth assessment report of the Intergovernmental Panel on Climate Change (IPCC). The RCP set consists of four scenarios (RCP2.6, RCP4.5, RCP6.0 and RCP8.5) each of which

* Corresponding author. Royal Netherlands Meteorological Institute, P.O. Box 201, 3730 AE De Bilt, Netherlands. Tel.: +31 30 2206392; fax: +31 30 2210407.
E-mail address: chuwah@knmi.nl (C. Chuwah).

1352-2310/$ – see front matter © 2013 Elsevier Ltd. All rights reserved.
http://dx.doi.org/10.1016/j.atmosenv.2013.07.008

describes a different trajectory for emissions of long-lived greenhouse gases (LLGHGs) and short-lived air pollutants, the corresponding concentration levels, land use and radiative forcing. Together the four RCPs span a range of possible climate forcings varying from 2.6 W m^{-2} to 8.5 W m^{-2} in 2100 (Van Vuuren et al., 2011a). It should be noted that the four RCPs have been produced by four different integrated assessment models (IAMs) (see Masui et al., 2011; Riahi et al., 2011; Thomson et al., 2011; Van Vuuren et al., 2011b).

The emissions trajectories of air pollutants are determined by three important factors: the level of economic activities, the assumed degree of air pollution control and the assumed level of climate policy (Van Vuuren et al., 2011a). The relationship with climate policy originates from the fact that LLGHGs and air pollutants have a number of common sources. As such, policies aimed at curbing LLGHGs often lead to reduction in air pollutants (e.g. Van Vuuren et al., 2008; Koornneef et al., 2010). In the RCPs, all modelling teams assumed that higher income levels lead to the implementation of more stringent air pollution control measures. Overall, this implies that in each RCP air pollutant emission factors gradually decline during the course of the century. Van Vuuren et al. (2011c) conclude that the RCP set shows a smaller range of possible outcomes with respect to air pollutant emissions than other scenario sets, such as the IPCC SRES scenarios (Nakićenović et al., 2000), used in Prather et al. (2003), and scenarios from the International Institute for Applied Systems Analysis (IIASA), utilized by Dentener et al. (2006) and Kloster et al. (2008). This narrow range may limit the use of the RCPs for projecting future changes in air quality and climate forcing from short-lived components.

Given the importance of the RCPs, the key research question that is addressed in this study is: what would be the possible ranges of future air pollutant emissions, associated concentrations and climate forcings if a wider range of air pollution assumptions is included. In order to systematically distinguish the impacts of climate policy (different LLGHG emission profiles corresponding to RCP forcing levels) and air pollution control, it is most interesting to investigate this within a single model framework. Therefore, we explore the impact of alternative assumptions regarding air pollutant emissions using a set of RCP-like scenarios developed using the IMAGE integrated assessment model. While these are RCP replications (designed in a different model framework), the exact reproduction is not important for answering the research questions listed above.

In the past, several studies have already analysed the implications of climate and air pollution policies on air pollutants (e.g. Kloster et al., 2008; Van Aardenne et al., 2010; Shindell et al., 2012; Bond et al., 2013). In general, these studies show that climate and air pollution policies implementation have co-benefits on air pollutant concentrations and climate forcing from short-lived components. We do add to this literature by the direct relation with the RCPs and the systematic framework of air pollution and climate policy scenarios described in the next section.

The paper is structured as follows: Sect. 2 describes the modelling system and the methods used to develop the new scenarios. In Sect. 3, we compare the evolution of the emissions and methane concentrations in our scenarios and the RCPs, and we present results for surface concentrations and radiative forcing. A discussion and conclusions of our results are given in Sect. 4.

2. Models and methods

The modelling framework used in this study is schematically illustrated in Fig. 1b and consists of the Integrated Model to Assess the Global Environment (IMAGE, Bouwman et al., 2006) and the atmospheric chemistry and transport model TM5 (Huijnen et al., 2010). A description of these models is included in the supplementary material.

The IMAGE model is used to develop a set of consistent scenarios (IM2.6-low, IM2.6-high, IM6.0-low and IM6.0-high). These scenarios explore the impact of very different assumptions in terms of both climate policy (IM2.6 versus IM6.0) and air pollution control (high and low variants, see Fig. 1a). The IM6.0-low scenario is an IMAGE variant of the RCP6.0 produced by the Asian-Pacific Integrated Model (AIM) leading to a 2100 forcing level of 6.0 W m^{-2}. For both climate scenarios, variants were made assuming air pollution control policies following similar assumptions as the RCPs (low) and an alternative scenario assuming no improvement in the implementation of air pollution control measures whatsoever (high). This hypothetical assumption forms an upper bound on possible emission trajectories, providing a natural reference level for the impact of air pollution policy. In reality, very high air pollution levels are likely to evoke a policy response, but the main purpose here is to provide an indication of the range of possible air pollution levels under different assumptions in the integrated assessment model IMAGE.

The TM5 model is used for a detailed grid-level representation of the atmospheric chemistry and to estimate the effect of future emission changes on the concentrations of air pollutants and aerosol optical depth, based on the present-day climate. Emission changes are the most important driver of changes in tropospheric ozone and aerosols in the coming decades. The effects of climate change are still very uncertain and model dependent, but are expected to be generally smaller (Stevenson et al., 2006; Lamarque et al., 2011; Fiore et al., 2012; Young et al., 2013). The model was driven by meteorological data from the ERA-Interim reanalysis (Dee et al., 2011) of the European Centre for Medium-Range Weather Forecasts (ECMWF). Simulations were carried out for the years 2005, 2020 and 2050, using meteorological fields for 2005.

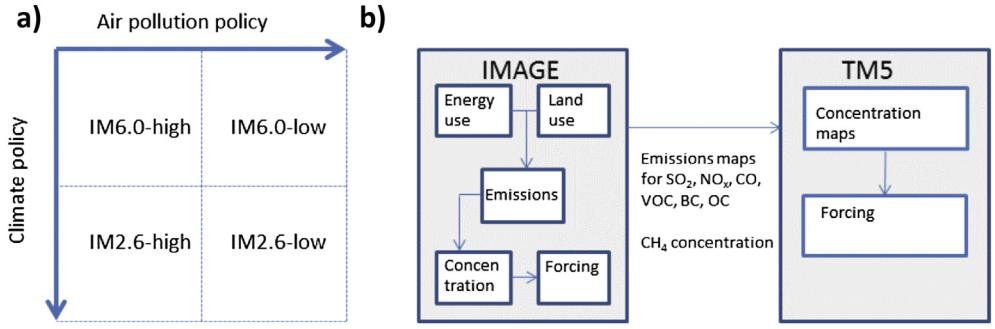

Fig. 1. (a) A matrix of the four IMAGE scenarios analysed in this study illustrating the different degrees of climate and air pollution policies. (b) The major components of the IMAGE and TM5 models and the IMAGE output variables used in TM5.

Based on the TM5 simulations, we recalculate the radiative forcing of aerosols and tropospheric ozone (see Sect. 2.2).

2.1. Scenarios development process

The scenarios used in this study are derived from the baseline scenario developed for the OECD Environmental Outlook (OECD, 2012). On the basis of the baseline, mitigation scenarios were developed targeting a 2100 radiative forcing level of 2.6 and 6.0 W m^{-2} (Fig. 1a). In the scenarios with stringent air pollution control (IM2.6-low and IM6.0-low), it is assumed that emission factors (emissions per unit activity per sector and fuel type) of air pollutants decline up to 2030 assuming implementation of current and planned air quality policies. After 2030, further abatement measures are implemented as a function of the increasing income levels by applying gross domestic product (GDP) thresholds for medium and advance levels of air quality control (Lucas et al., 2007; Van Vuuren et al., 2007). In the two high scenarios labelled IM2.6-high and IM6.0-high, the implementation of current and planned air quality legislations is presumed till 2010 after which we assume constant emission factors onwards. In summary, the two climate policy variants (IM2.6 and IM6.0) differ with respect to energy use and land use, while the air pollution variants (high and low) refer to different emission factors.

2.2. Radiative forcing

In the design of the four scenarios, the radiative forcing (RF) levels are calculated in IMAGE. We also include a post-calculation of the aerosol and tropospheric ozone forcing using the TM5 output. In both cases, the calculations are based on the MAGICC6 approach (Appendix A; Meinshausen et al., 2011a). In the case of ozone (O_3), a mean forcing efficiency of 0.042 W m^{-2} DU^{-1} is used to convert the simulated tropospheric burden changes to RFs, in agreement with the recent estimate by Stevenson et al. (2013). Monthly mean tropospheric O_3 columns are determined using the 150-ppb O_3 level to define the tropopause height. This is done using the fixed 2005 monthly mean O_3 mixing ratio fields in the demarcation of the tropopause for all scenarios. With respect to methane, we calculate the RF from the concentration using the simplified expression applied in MAGICC (see e.g. Meinshausen et al., 2011a).

Our projections of changes in the RF by aerosols include only contributions from direct radiative effects. The chemical composition and consequently the optical properties of the different aerosol types might change as a result of climate change, but such climate-driven changes are not considered in this study. It is therefore justified to assume a linear relationship between the direct radiative effect of an individual aerosol component and its optical depth. Thus, to estimate the future RFs of the various aerosol components we make use of the present-day RF calculations from the GISS model E simulations by Hansen et al. (2005) and apply a simple linear scaling based on the anthropogenic contributions to the aerosol optical depths (AODs) of the various components simulated in TM5. This procedure is similar to the method applied in MAGICC6, but we use scaling ratios defined in terms of optical depths at 550 nm instead of emissions of aerosols or aerosol precursor gases.

As in MAGICC6, we apply a hemispheric approach wherein we apply separate scaling factors over the land and ocean areas in both hemispheres. At this aggregated level, potential mismatches related to different spatial distributions of the AODs in TM5 and

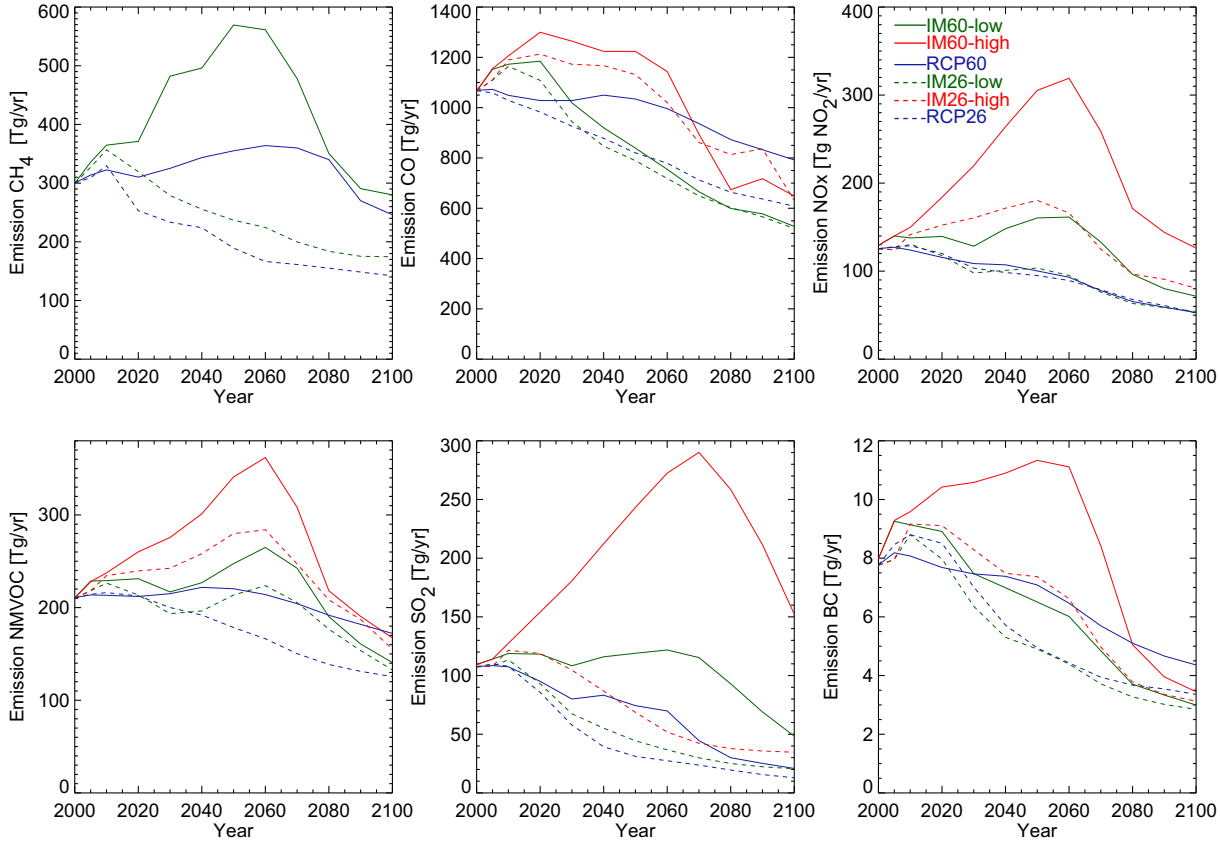

Fig. 2. Annual total anthropogenic emissions of CH_4, CO, NO_x, NMVOC, SO_2, and BC in the new IMAGE scenarios and the corresponding RCPs. Emissions from biomass burning are included in the totals.

GISS (e.g. due to different emission distributions) will largely average out. Thus, the global mean future radiative forcing per aerosol component i is calculated as

$$RF_i(\text{year}) = \overline{RF_{i,r}^{GISS} \times \frac{AOD_{i,r}^{anthro}(\text{year})}{AOD_{i,r}^{anthro}(2005)}}.$$

Here $RF_{i,r}^{GISS}$ is the present-day radiative forcing estimate for component i and region r from Hansen et al. (2005), $AOD_{i,r}^{anthro}$ is the anthropogenic AOD of component i averaged over region r, and the overbar represents the area weighted averaging over the four regions (land and ocean in both hemispheres). It is important to note that the radiative forcing from tropospheric ozone and aerosols varies regionally (e.g. Stevenson et al., 2013; Myhre et al., 2013). The aggregated approach described here does not give any information about the magnitude of these regional variations.

3. Results

3.1. Emission projections

Fig. 2 shows the pathways for the global total emissions of methane (CH_4), carbon monoxide (CO), nitrogen oxides (NO_x), non-methane volatile organic compounds (NMVOCs), sulphur dioxide (SO_2), and black carbon (BC). Regional totals for four main industrialized regions, viz. North America (NA), Europe (EU), East Asia (EA) and South Asia (SA), are presented in the Supplementary material. The definition of these regions follows the definition applied by the Task Force on Hemispheric Transport of Air Pollution (HTAP; see Wild et al., 2012).

The emission pathways of individual components in the scenarios analysed here are somewhat different from the RCPs (Fig. 2). The differences between the RCP2.6 and IM2.6-low scenarios are small and originate from the updated baseline and model version (for instance, more rapid baseline growth in China has been assumed (OECD, 2012)). The differences between the IM6.0-low and RCP6.0 scenarios are larger as they are produced by two different IAMs (IMAGE and AIM). The AIM model produces lower methane emissions in Asia than IMAGE (Figs. S4 and S5). This is caused by different assumptions on activity levels for agriculture (livestock and rice) and energy production (coal mining). Both scenarios are, however, bounded by the radiative forcing target which means that for the combination of greenhouse gases a similar profile emerges.

In the IM2.6-high and IM6.0-high scenarios, the emissions of CO_2, CH_4, and other LLGHGs are the same as in the corresponding low air pollution scenarios, but air pollutant emissions are considerably higher due to the assumptions on emission factors. Clear differences can be noted in SA and EA (see Figs. S4 and S5), where rapid growth in economic activities leads to a corresponding increase in pollutant emissions, if air pollution policies are not tightened. Nevertheless, even in the high emission scenarios emissions mostly decrease in the second half of the century as a result of reduced direct use of fossil fuels (for instance, in transport, the scenarios assume increased use of hydrogen power resulting in much lower emissions than with oil-based fuels).

3.2. Methane concentrations

Projections for methane concentrations are shown in Fig. 3. The concentrations in IM2.6-low are slightly higher than in the RCP2.6 as result of changes in the IMAGE model version and baseline assumptions (see Fig. 2). The higher concentrations in IM6.0-low compared to RCP6.0 are also a result of higher methane emissions (and reflect the differences in the AIM and IMAGE projections). Comparing the high and low air pollution scenarios, we find lower concentrations in the high scenario variants, especially in 2050. In other words, the effect of the higher NO_x emissions dominates over the opposing effects of the higher CO and NMVOC emissions. Higher NO_x concentrations in the high air pollution scenarios lead to enhanced recycling of the hydroxyl radical (OH) and thus to higher abundances of OH in the troposphere. This tends to reduce the methane lifetime compared to the low air pollution scenarios, which results in lower methane concentrations despite the fact that the methane emissions are the same in both scenario variants.

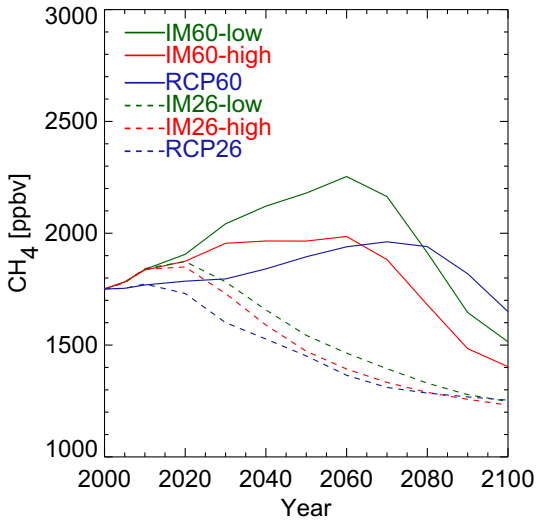

Fig. 3. Global mean methane concentrations in the new IMAGE scenarios and the corresponding RCPs.

3.3. Future air quality

Annual mean surface concentrations of ozone, sulphate and black carbon simulated with TM5 are presented for 2020 and 2050, and compared to the reference year 2005.

3.3.1. Surface ozone concentrations

The projected surface ozone concentrations vary over a very wide range as they are found to be sensitive to the implementation of air quality and climate policies, even in the short term (Figs. 4 and 5). In the IM6.0-high scenario, the annual mean ozone concentrations are projected to increase over almost the entire globe. In 2050, increases as high as 30 ppbv are observed near the Indian subcontinent. Some exceptions are noted where concentrations decrease, most notably in the northeastern part of China. With low emission factors (IM6.0-low) the situation changes: now ozone concentrations are projected to decrease in the eastern United States, parts of the Mediterranean, the Black Sea, Kazakhstan and surrounding regions, and, in 2050, in regions of the Amazon and Central Africa where biomass burning plays a dominant role (see Fig. 4). In the latter regions the differences between the high and low scenario variants are mostly due to the influence from the surrounding regions, as the emissions from biomass burning are the same in both variants.

Interestingly, in eastern China ozone concentrations are projected to decrease in both IM6.0 scenarios despite increases in NO_x emissions. This indicates that this region is in a hydrocarbon-limited regime wherein surface ozone production is limited by NMVOCs. Local titration of ozone mainly during winter may also

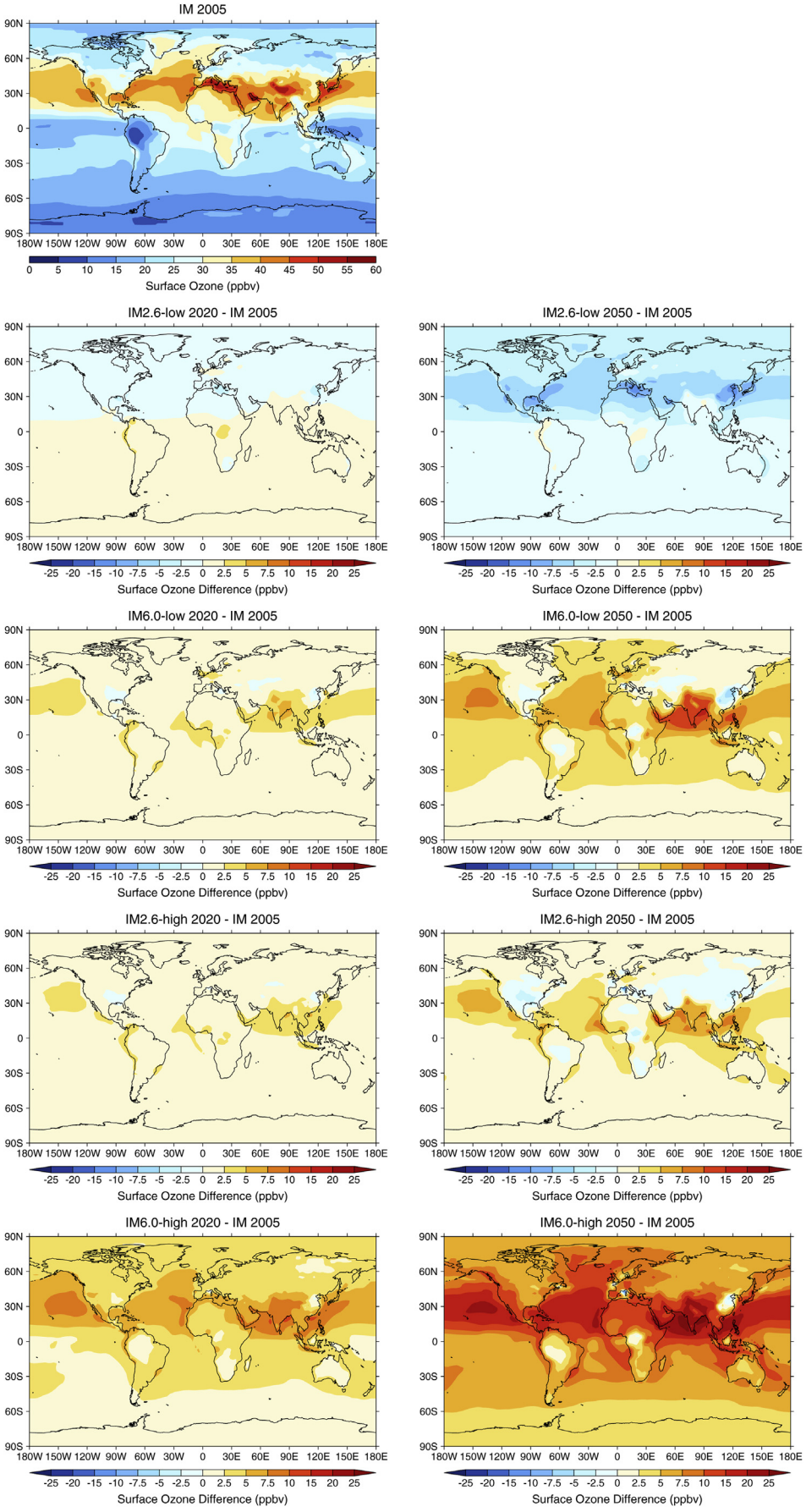

Fig. 4. Simulated annual mean surface ozone concentrations in 2005 and the changes in 2020 and 2050 relative to 2005 for the different scenarios.

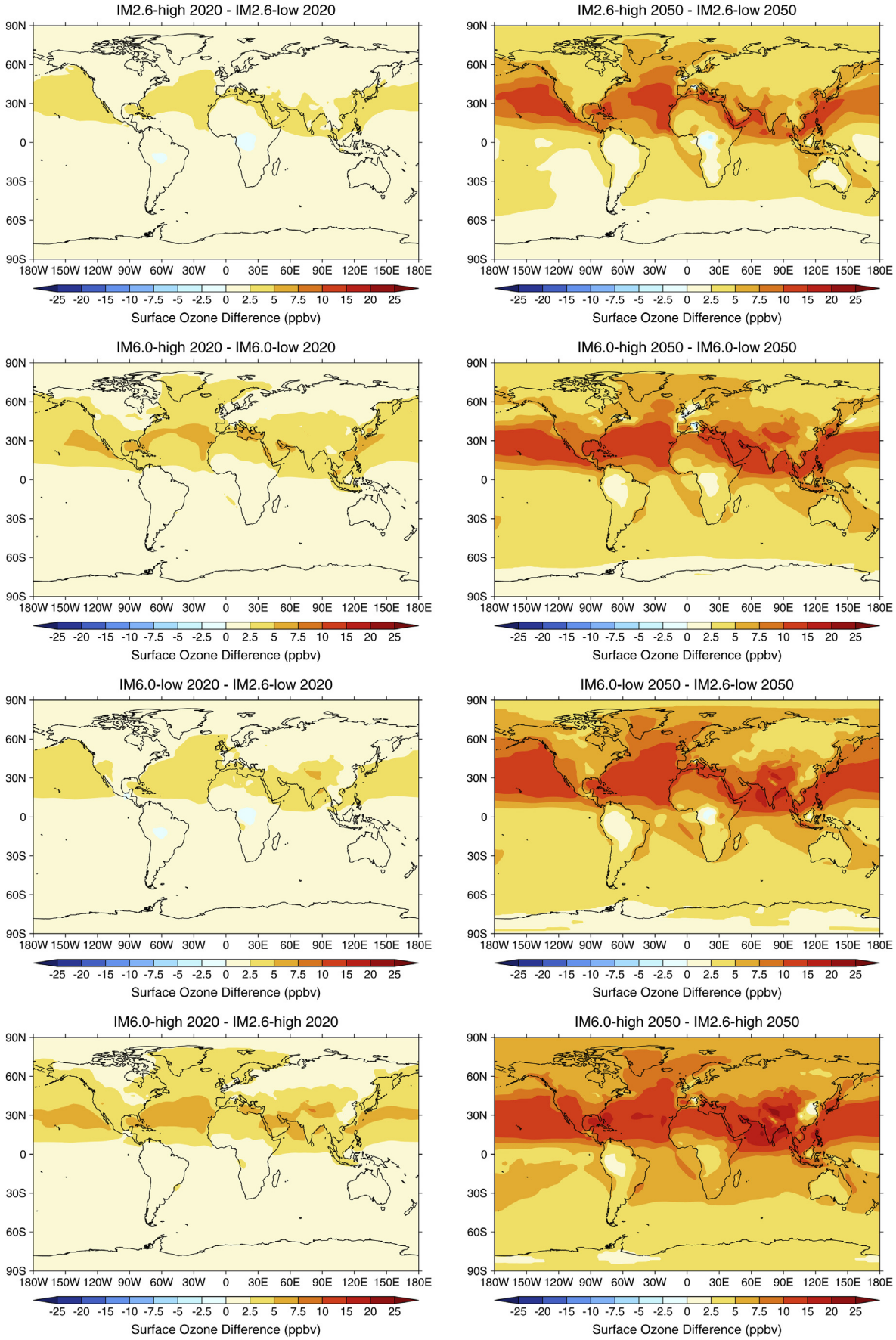

Fig. 5. Differences in the annual mean surface ozone concentration between the high and low air pollution scenarios (top panels) and the weak and strong climate policy scenarios (bottom panels) for 2020 and 2050.

play a role in the observed decrease in surface ozone over eastern China (see also Pozzer et al., 2012).

In the IM2.6-high scenario, the ozone concentrations will first increase in most parts of the world, but by the middle of the century decreases are simulated in large parts of the continents, including the United States, China, and South Africa. In the lowest emission scenario (IM2.6-low), the ozone concentrations are still projected to increase in 2020 in most of the Southern Hemisphere (SH) as well as in India and Southeast Asia. In contrast, the IM2.6-low scenario leads to decreased concentrations in large parts of the Northern Hemisphere (NH), as a result of reductions in ozone precursor emissions in the industrialized regions. In the longer term (2050), the ozone concentrations in this mitigation scenario will be reduced over almost the entire globe with the strongest reductions reaching 10 ppbv at northern mid-latitudes. Regionally averaged annual mean concentration values for NA, EU, EA and SA and the different scenarios are presented in Fig. 6. The corresponding global mean values are given in the Supplementary material (Table S1).

The differences in ozone concentrations as a result of the assumed differences in air pollution control and those in climate policy are qualitatively similar (Fig. 5). The largest differences are observed in the NH subtropics and mid-latitudes. As expected, air pollution control is most effective in reducing the ozone concentrations when there is less climate policy in place. Similarly, the co-benefits of climate policy for the ozone air quality are largest when air pollution control is weak. However, the highest future reductions in ozone concentrations are achieved under the IM2.6-low scenario, emphasizing the importance of the co-benefits of climate policy for ozone concentrations.

3.3.2. Surface concentrations of sulphate

The results for surface concentration of sulphate (SO_4) depend on the region, time period and scenario. An increase is observed in the short term (2020) in all four scenarios in the Asian regions, mainly as a result of increasing energy demand and reliance on coal. At the same time, in all scenarios in 2020 a decrease is observed for North America, the North Atlantic, western Europe, and Australia, mainly due to SO_2 emission reductions achieved in the power sector (Fig. 7).

In the highest emission scenario (IM6.0-high), the increase in concentration continues in the period up to 2050 in many developing regions (Middle East, Asia, Africa, and South America, and over the tropical and subtropical oceans) (see also Fig. 6 for the NA, EU, EA and SA regions). The largest increases are projected in southern and eastern Asia, where annual mean concentrations in some places increase by more than 25 μg m^{-3} in 2050. In contrast, under IM6.0-low in 2050 the sulphate concentrations at northern mid- and high latitudes are reduced, even in the northern parts of China. In IM2.6-high the concentrations in 2050 decline in most parts of the world except in the north of India, parts of central Africa and the west coast of Latin America. In IM2.6-low the increases in these regions are further reduced, while the concentrations in eastern China are reduced by up to about 5 μg m^{-3}.

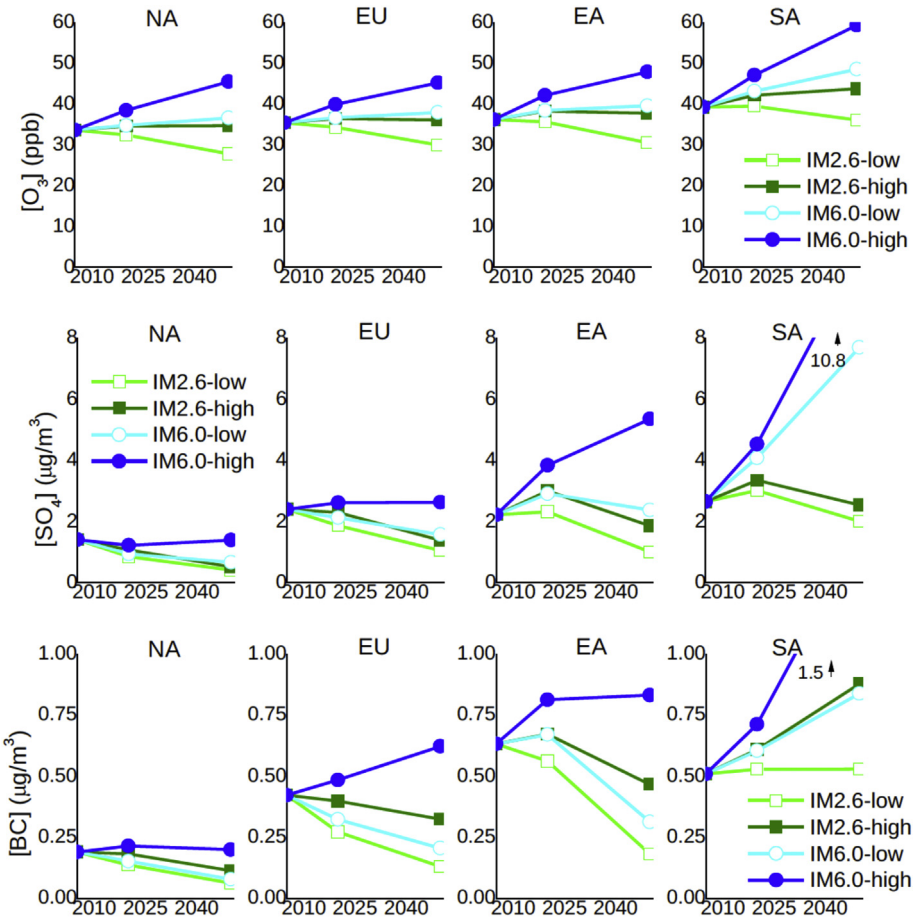

Fig. 6. Simulated regional and annual mean surface ozone, sulphate and black carbon concentrations in 2005, 2020 and 2050 for North America (NA) (60°W–125°W × 15°N–55°N), Europe (EU) (10°W–50°E × 25°N–65°N), East Asia (EA) (95°E–160°E × 15°N–50°N) and South Asia (SA) (50°E–95°E × 5°N–35°N).

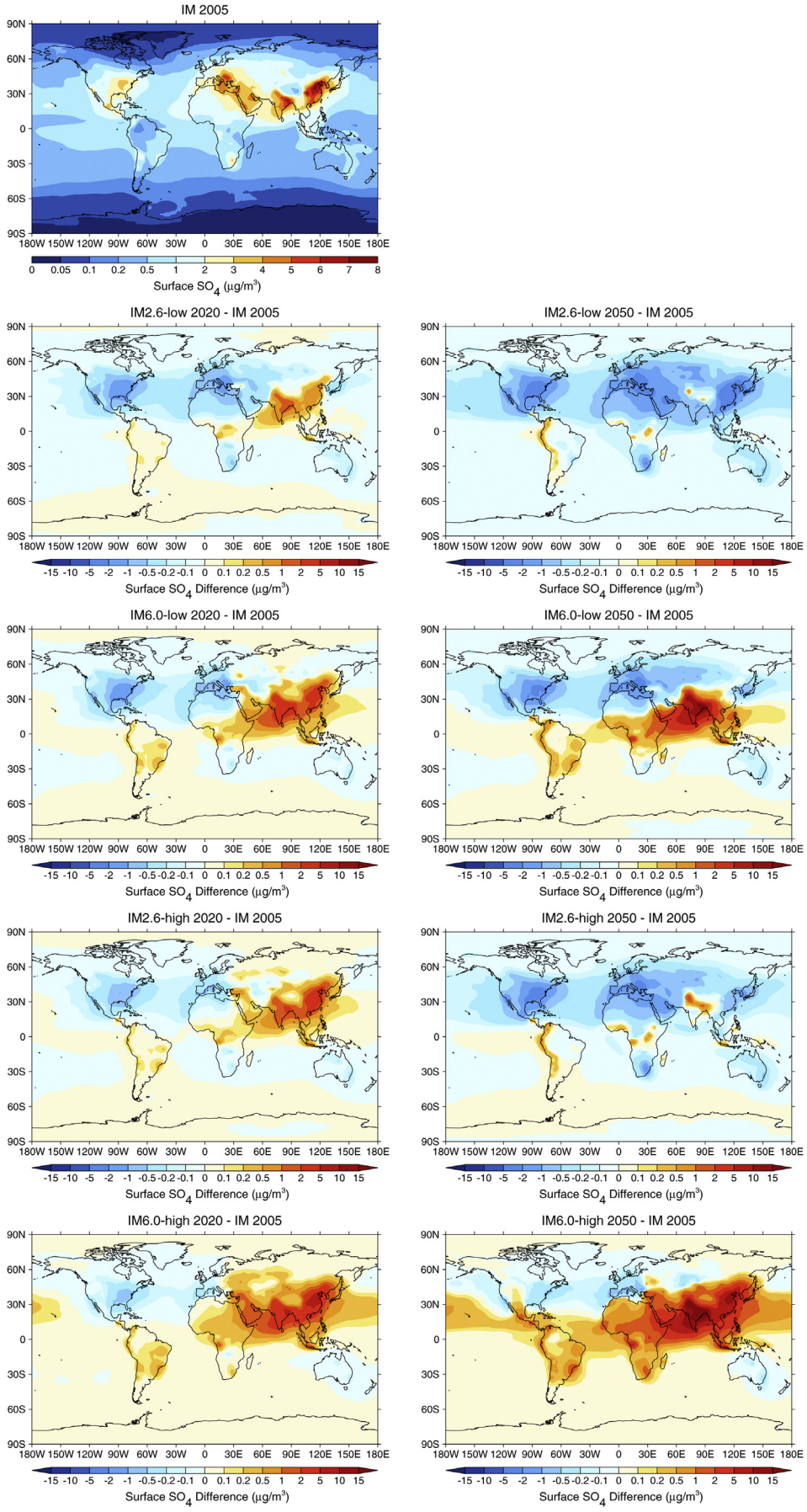

Fig. 7. Simulated annual mean surface SO_4 concentrations in 2005 and the changes in 2020 and 2050 relative to 2005 for the different scenarios.

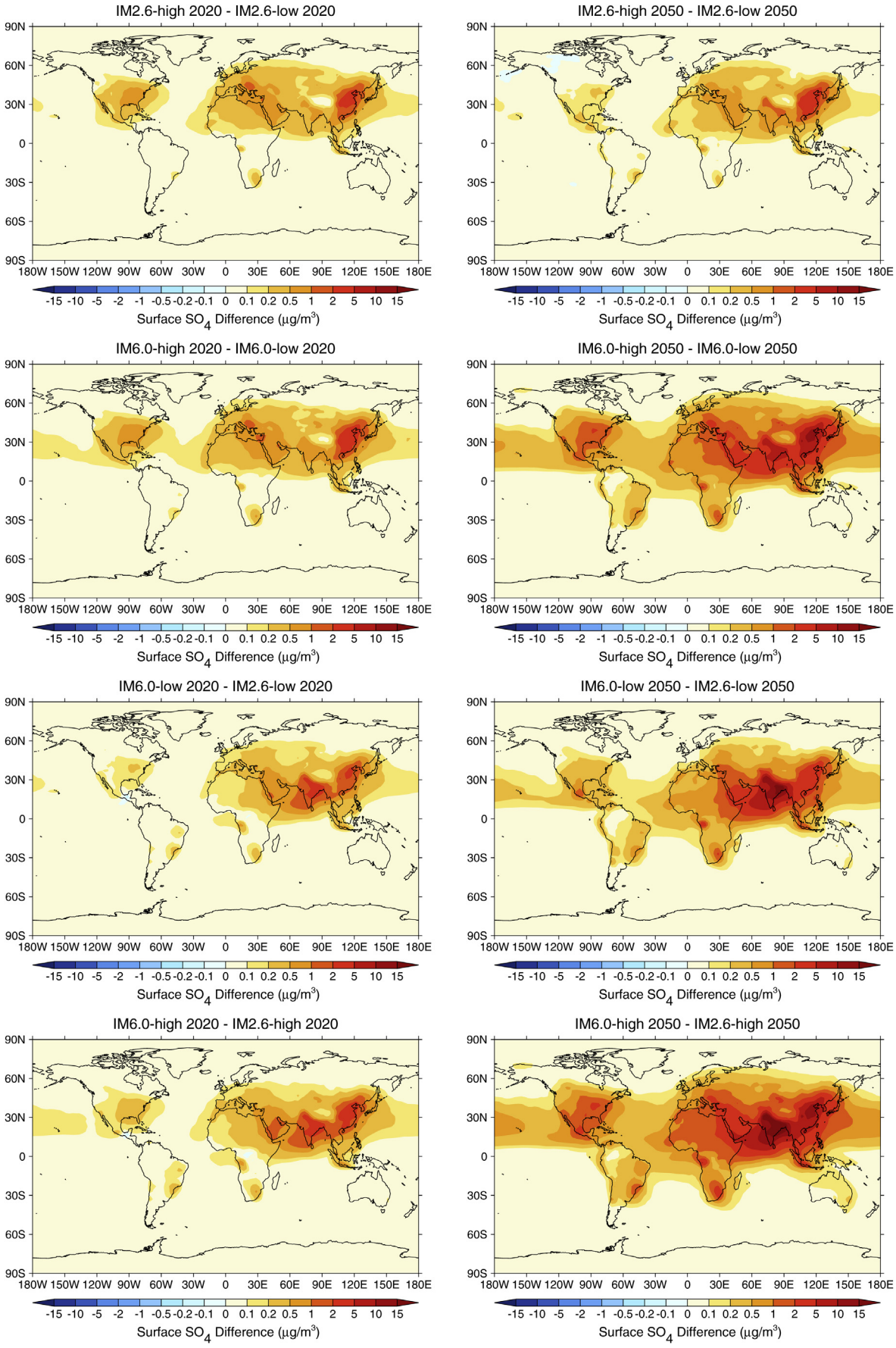

Fig. 8. Differences in the annual mean surface SO_4 concentrations between the high and low air pollution scenarios (top panels) and the weak and strong climate policy scenarios (bottom panels) for 2020 and 2050.

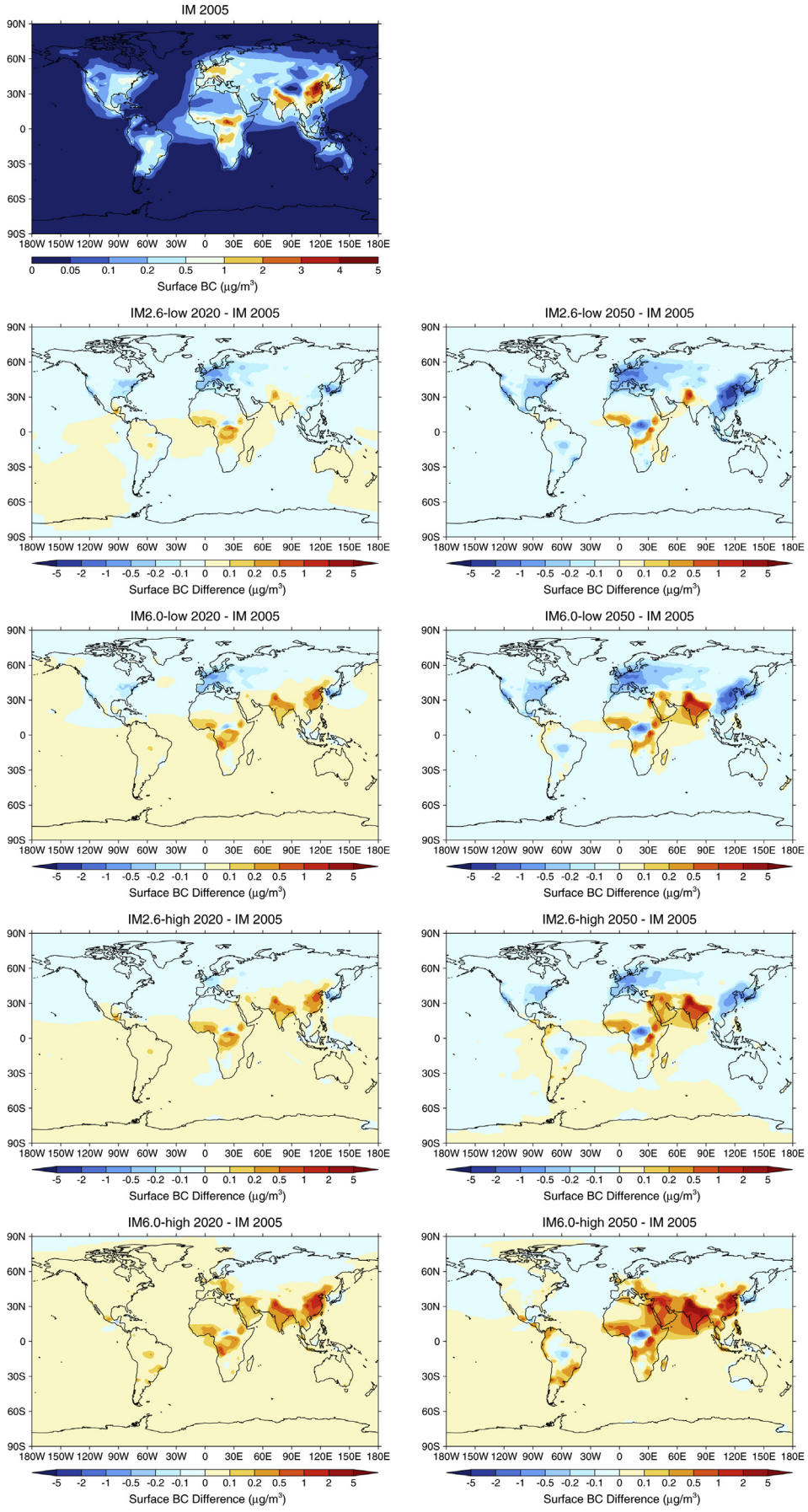

Fig. 9. Simulated annual mean surface BC concentrations in 2005 and the changes in 2020 and 2050 relative to 2005 for the different scenarios.

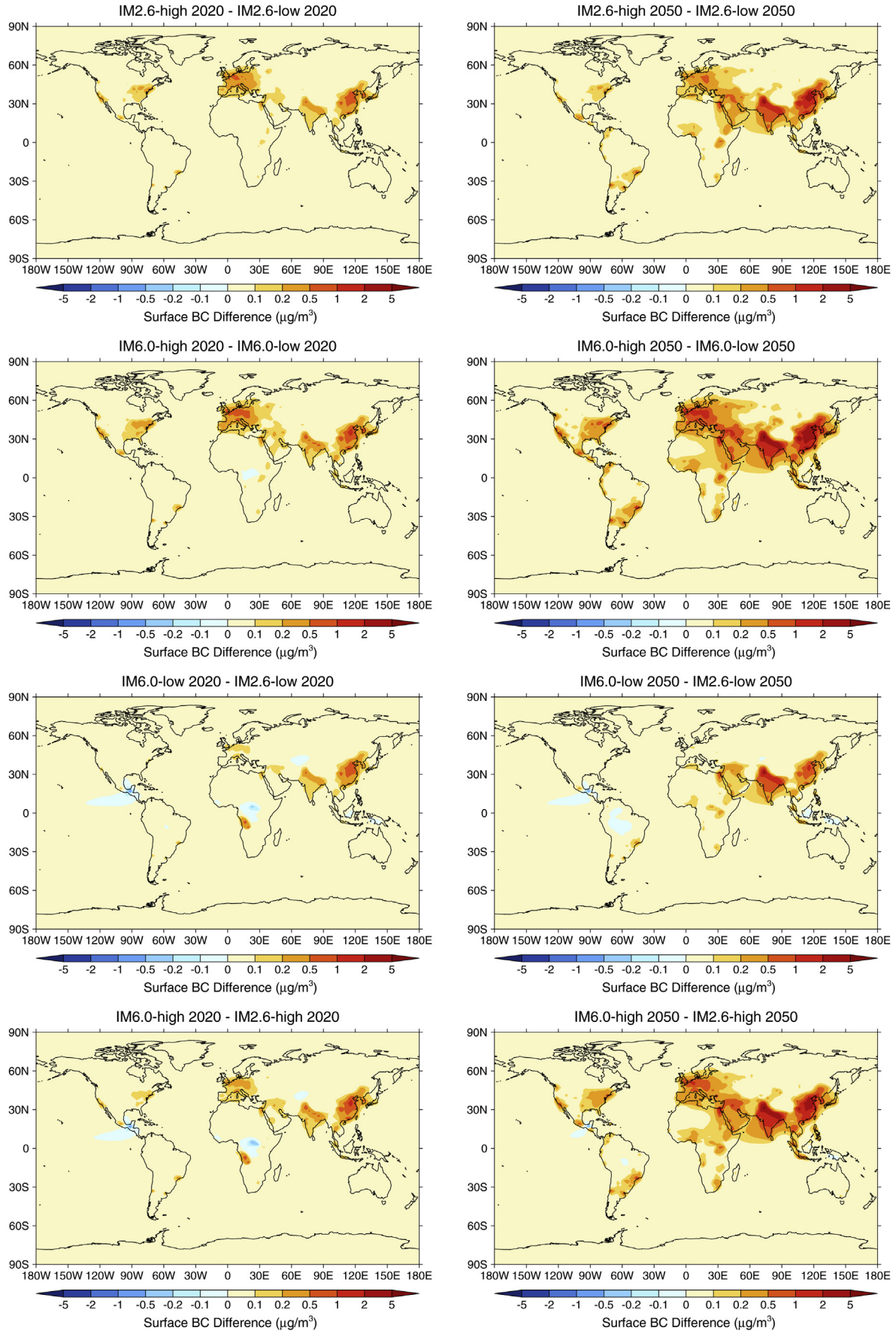

Fig. 10. Differences in the annual mean surface BC concentrations (μg m^{-3}) between the high and low air pollution scenarios (top panels) and the weak and strong climate policy scenarios (bottom panels) for 2020 and 2050.

Clearly, the impact of air pollution policy assumptions on sulphate concentrations is less in the IM2.6 than in the IM6.0 scenario (Fig. 8). The reason is that a large part of the SO_2 emissions are caused by coal fired power plants, which are progressively being phased out in the 2.6 W m^{-2} scenario. The largest effects are observed in India and eastern China, where a rapid increase in energy demand and a high dependence on coal lead, in the absence of further control, to high SO_2 emissions. Significant effects can also be observed in the Middle East, parts of Eastern Europe, the Mediterranean region, the eastern US, Mexico, and parts of Latin America and Africa.

It should be noted that the assumptions of the IM6.0-high scenario lead to extremely high sulphate concentrations in Asia, as a result of increasing coal use in this region. This shows that further tightening of air pollution standards in Asia is needed.

3.3.3. Surface concentrations of black carbon

In the highest emission scenario (IM6.0-high) the surface concentrations of black carbon (BC) strongly increase in many world regions, including the Middle East, Eastern Europe, the eastern US, and in parts of Latin America, Africa and especially eastern China and India (Fig. 9). In contrast, in the IM6.0-low and IM2.6-high scenarios BC concentrations are reduced in North America and Europe, and by the middle of the century also in China. In the lowest emission scenario (IM2.6-low), the BC concentrations are reduced in most parts of the world, even in China in 2020. However, increased concentrations are still observed in 2050 in this scenario in northern India and Pakistan and parts of Africa. Fig. 6 shows the regionally averaged BC concentrations for NA, EU, EA and SA.

As for ozone, starting from the IM6.0-high scenario air pollution and climate policies have quantitatively similar effects on the BC concentrations, both in 2020 and 2050 (Fig. 10). Large reductions of up to about 5 μg m^{-3} can be achieved by both types of policies in the most polluted parts of India and China. Indeed, the regional total BC emissions in SA and EA follow similar pathways under the IM6.0-low and IM2.6-high scenarios (see Figs. S4 and S5). The implementation of air pollution control is also effective in reducing the BC concentrations in case of the stringent climate policy scenario (IM2.6-high scenario). We note that in our modelling study the co-benefits of climate policy are relatively small if climate mitigation measures are introduced in a situation of already existing stringent air pollution policies, especially in Europe and the United States. However, the co-benefits are much more important in achieving further improvement in air quality in India and China.

3.4. Future radiative forcings

The global mean radiative forcings are estimated from the IMAGE methane concentrations and TM5 ozone concentrations and component-specific aerosol optical depths and include only the direct radiative effects (Table 1).

For methane, we project a slight increase in the RF in 2020 in all scenarios. However, the projected radiative forcing in the longer term clearly depends on whether stringent climate policies are introduced (increases in IM6.0 and a decrease in IM2.6). As observed in Sect. 3.2, the methane RFs are lower in the high than in the corresponding low air pollution scenarios, especially in 2050.

The different scenarios for ozone lead to very different forcings. For the IM2.6-low scenario we find a negligible change in 2020 and a reduction of 0.12 W m^{-2} in 2050 compared to today. In all other scenarios, the global mean ozone RF is expected to increase. The strongest increases are produced in the IM6.0 scenarios, especially in the high air pollution variant where the ozone RF is increased by 0.34 W m^{-2} in 2050.

The direct RF contributions from individual aerosol components are projected to go in very divergent directions as a function of the policy assumptions. In IM2.6-low, the sulphate cooling effect on the climate is projected to decrease by 0.08 W m^{-2} in 2020 and by 0.31 W m^{-2} in 2050 (i.e. the negative forcing becomes smaller). Also if the stringent air pollution policies are dropped, the cooling by sulphate is reduced by 0.19 W m^{-2} in 2050 (but there is a small peak in 2020). Finally, in the IM6.0 scenarios the sulphate cooling is enhanced both in 2020 and 2050 (by maximally 0.84 W m^{-2} in IM6.0-high in 2050).

For black carbon (BC), both climate and air pollution policies are relevant in determining the final change in forcing. In the IM2.6-low scenario the warming effect of BC is projected to decrease by 0.05 W m^{-2} in 2020 and by 0.22 W m^{-2} in 2050. Conversely, in both the IM2.6-high and IM6.0-low scenarios, the BC RF first peaks in 2020 and slightly declines in 2050. Finally, in the IM6.0-high scenario the warming by BC is projected to increase by 0.15 W m^{-2} in 2020 and by 0.39 W m^{-2} in 2050.

For organic carbon (OC), much smaller changes in the RF are projected than for sulphate and BC (Table 1). The abundance of the semi-volatile ammonium-nitrate aerosol may change regionally in response to local changes in ammonia (NH_3) emissions and sulphate concentrations. The effect on the global mean RF is uncertain, but for our scenarios we estimate it to be smaller than for the other components. The total aerosol direct RF is therefore determined by the changes in the contributions from sulphate and BC. Changes in the cooling by sulphate are generally dominant, but are still partly compensated by the changes in the warming by BC. Thus, the changes in the combined aerosol RF are much smaller than in the separate contributions from sulphate and BC. As a result, the aerosol RF remains close to present-day levels in 2020. For 2050 the aerosol RF is projected to increase in the IM2.6 scenarios (by 0.12 W m^{-2} in IM2.6-low and by 0.18 W m^{-2} in IM2.6-high), and to decrease in the IM6.0 scenarios (by 0.22 W m^{-2} in IM6.0-low and by 0.44 W m^{-2} in IM6.0-high).

Table 1
Estimated global mean direct radiative forcings (W m^{-2}) of methane, tropospheric ozone and aerosols in 2020 and 2050 relative to 2005.

Tracers	IM2.6 Low 2020	IM2.6 High 2020	IM6.0 Low 2020	IM6.0 High 2020	IM2.6 Low 2050	IM2.6 High 2050	IM6.0 Low 2050	IM6.0 High 2050
CH_4	0.034	0.026	0.045	0.034	−0.091	−0.12	0.14	0.066
O_3	−0.001	0.040	0.066	0.15	−0.12	0.022	0.13	0.34
SO_4	0.081	−0.045	−0.055	−0.22	0.31	0.19	−0.20	−0.84
OC	−0.003	−0.009	−0.013	−0.018	0.038	0.031	0.016	0.003
BC	−0.046	0.047	0.032	0.15	−0.22	−0.039	−0.037	0.39
$CH_4 + O_3$	0.033	0.065	0.11	0.18	−0.21	−0.098	0.27	0.41
Aerosol	0.032	−0.006	−0.036	−0.090	0.12	0.18	−0.22	−0.44
Total RF	0.066	0.059	0.076	0.090	−0.082	0.081	0.054	−0.033

Interestingly, the impacts described above also lead to strong cancellation of the contributions of methane, ozone and aerosols to the total global mean RF. The absolute change in the total RF of these components is maximally 0.09 W m^{-2} (IM6.0-high in 2020).

Similarly, the global climate effect of worldwide implementation of air pollution control is determined by the balance between the reduced warming by ozone and BC versus the reduced cooling by sulphate and the enhanced warming by methane. In both climate scenarios the net effect on the total global mean RF in 2020 is small. In the longer term, the reduced cooling by sulphate dominates in the IM6.0 scenario, whereas the reduced warming by ozone and BC dominates in the IM2.6 scenario. As a result, the global mean RF in 2050 changes by +0.09 W m^{-2} in IM6.0 and by −0.16 W m^{-2} in IM2.6 as a result of air pollution control. It is important to emphasize that the cancellation of the contributions of the individual components to the RF may not occur at regional and local scales.

4. Discussion and conclusions

This study has explored the impact of different assumptions regarding air pollution control in RCP-like scenarios on both air quality and direct radiative forcing of climate in 2020 and 2050. In our scenarios, air pollution control and climate mitigation policies both have large-scale effects on the concentrations of air pollutants, often of similar magnitude. The scenario with both stringent climate policy and air pollution control policies, therefore, results in the lowest concentrations. The results also show that in our modelling study the co-benefits of climate policies for air quality become lower for higher levels of air pollution control. Clearly, this study indicates that while climate mitigation policies do have important co-benefits for air quality, they alone are not enough to resolve air quality problems. The results confirm that the range of air pollutant emissions and concentration levels associated with the RCPs is indeed constrained by the assumed air pollution policies in these scenarios. If no further air pollution policies would be implemented, air pollutant concentration levels could be considerably higher than in the RCPs, especially in Asia.

The co-benefits of worldwide implementations of air pollution control policies for mitigating global warming was analysed in terms of its effect on the direct radiative forcing of methane, tropospheric ozone, and aerosols (sulphate, BC and OC). Air pollution control leads to substantially reduced warming by ozone at regional to continental scales, which at the global scale is partially compensated by increased warming by methane. Also, we project strong reductions in the cooling by sulphate and in the warming by BC, and much smaller changes in the RF by OC. The combined effect of air pollution policy on the global mean direct RF of the aerosols together is a small positive forcing in both climate scenarios in 2020. In the longer term (2050) it leads to a small negative RF by aerosols in the 2.6 W m^{-2} scenario due to reductions in BC, and a substantial positive RF of 0.22 W m^{-2} by aerosols in the 6.0 W m^{-2} scenario, where air pollution control will significantly reduce sulphate emissions, especially in Asia. The combined global mean RF from methane, ozone and aerosols together is hardly affected by air pollution policies in the short term. By the middle of the century, air pollution control is projected to change the total global mean RF by +0.09 W m^{-2} in the 6.0 W m^{-2} scenario, mostly due to reductions in the sulphate RF, and by −0.16 W m^{-2} in the 2.6 W m^{-2}.

The projections presented in this study are based on a number of assumptions. First, the methane concentrations pathways calculated in the IMAGE model are based on the parameterization applied in MAGICC6, which is based on a chemistry transport model intercomparison study performed for the IPCC Third Assessment Report (Ehhalt et al., 2001). Recently, Prather et al. (2012) presented improved methane concentration projections and associated uncertainties for the RCP emission pathways and compared their results with the official RCP concentration projections based on MAGICC6 (Meinshausen et al., 2011b). They found very good agreement for both RCP4.5 and RCP6.0, but concluded that MAGICC6 based concentration projections for RCP2.6 and RCP8.5 are at the high resp. the low end of their range of uncertainty.

We also applied the same meteorological data based on the ERA-Interim reanalysis in our TM5 simulations for the future and the present day. In reality, the future climate will change depending on the scenario assumed for emissions and land use, and future changes in meteorological parameters are expected to have an effect on the surface concentrations of air pollutants. Also, natural emissions of ozone and aerosol precursors are likely to evolve differently under future climatic conditions. However, the impacts of these anticipated future changes are still highly uncertain.

Furthermore, our estimates of the future changes in the direct RFs of the various aerosol components are based on the scaling approach described in Sect. 2.2, which involves aggregation of the simulated aerosol optical depth fields to sufficiently large scales. It should also be noted that our RF estimates don't include any indirect aerosol effects. Including those would make the sulphate effects relatively more important.

Compared to the RCP set of scenarios, the scenarios presented in this study give a much broader range of possible outcomes with respect to the future evolution of air pollutants. It is imperative to emphasize that though the RCPs include short-lived tracers and aerosols, they were not designed to assess future changes in air quality. Instead, they were produced to assess how different climate forcing targets can be reached by the end of the century, while assuming a continuation of the current trend towards more stringent air pollution control. This paper is meant to explore the potential impacts of varying air pollution policies. In this light, integrated emission scenarios focussing on short lived components as presented in this study are required to make representative projections of future changes in air quality and climate forcing.

Acknowledgements

This work is part of the research programme 'Feedbacks in the climate system', which is financed by the Netherlands Organisation for Scientific Research (NWO).

Appendix A. Supplementary data

Supplementary data related to this article can be found at http://dx.doi.org/10.1016/j.atmosenv.2013.07.008.

References

Bond, T.C., Doherty, S.J., Fahey, D.W., Forster, P.M., Berntsen, T., DeAngelo, B.J., Flanner, M.G., Ghan, S., Kärcher, B., Koch, D., Kinne, S., Kondo, Y., Quinn, P.K., Sarofim, M.C., Schultz, M.G., Schulz, M., Venkataraman, C., Zhang, H., Zhang, S., Bellouin, N., Guttikunda, S.K., Hopke, P.K., Jacobson, M.Z., Kaiser, J.W., Klimont, Z., Lohmann, U., Schwarz, J.P., Shindell, D., Storelvmo, T., Warren, S.G., Zender, C.S., 2013. Bounding the role of black carbon in the climate system: a scientific assessment. Journal of Geophysical Research 118, 1–173.

Bouwman, A.F., Kram, T., Klein Goldewijk, K., 2006. Integrated Modelling of Global Environmental Change. An Overview of IMAGE 2.4. Netherlands Environmental Assessment Agency (MNP), Bilthoven, The Netherlands.

Dee, D.P., Uppala, S.M., Simmons, A.J., Berrisford, P., Poli, P., Kobayashi, S., Andrae, U., Balmaseda, M.A., Balsamo, G., Bauer, P., Bechtold, P., Beljaars, A.C.M., van de Berg, L., Bidlot, J., Bormann, N., Delsol, C., Dragani, R., Fuentes, M., Geer, A.J., Haimberger, L., Healy, S.B., Hersbach, H., Hólm, E.V., Isaksen, L., Kållberg, P., Köhler, M., Matricardi, M., McNally, A.P., Monge-Sanz, B.M., Morcrette, J.-J., Park, B.-K., Peubey, C., De Rosnay, P., Tavolato, C., Thépaut, J.-N., Vitart, F., 2011. The ERA-interim reanalysis: configuration and performance of the data

assimilation system. Quarterly Journal of the Royal Meteorological Society 137, 553–597.
Dentener, F., Stevenson, D., Ellingsen, K., van Noije, T., Schultz, M., Amann, M., Atherton, C., Bell, N., Bergmann, D., Bey, I., Bouwman, L., Butler, T., Cofala, J., Collins, B., Drevet, J., Doherty, R., Eickhout, B., Eskes, H., Fiore, A., Gauss, M., Hauglustaine, D., Horowitz, L., Isaksen, I.S.A., Josse, B., Lawrence, M., Krol, M., Lamarque, J.F., Montanaro, V., Müller, J.F., Peuch, V.H., Pitari, G., Pyle, J., Rast, S., Rodriguez, J., Sanderson, M., Savage, N.H., Shindell, D., Strahan, S., Szopa, S., Sudo, K., Van Dingenen, R., Wild, O., Zeng, G., 2006. The global atmospheric environment for the next generation. Environmental Science and Technology 40, 3586–3594.
Ehhalt, D., Prather, M.J., Dentener, F., Derwent, R., Dlugokencky, E., Holland, E., Isaksen, I., Katima, J., Kirchhoff, V., Matson, P., Midgley, P., Wang, M., 2001. Atmospheric chemistry and greenhouse gases. In: Houghton, J.T., Ding, Y., Griggs, D.J., Noguer, M., van der Linden, P.J., Dai, X., Maskell, K., Johnson, C.A. (Eds.), Climate Change 2001: the Scientific Basis. Contribution of Working Group I to the Third Assessment Report of the Intergovernmental Panel on Climate Change. Cambridge University Press, Cambridge, United Kingdom and New York, NY, USA, pp. 239–287.
Fiore, A.M., Naik, V., Spracklen, D.V., Steiner, A., Unger, N., Prather, M., Bergmann, D., Cameron-Smith, P.J., Cionni, I., Collins, W.J., Dalsøren, S., Eyring, V., Folberth, G.A., Ginoux, P., Horowitz, L.W., Josse, B., Lamarque, J.-F., MacKenzie, I.A., Nagashima, T., O'Connor, F.M., Righi, M., Rumbold, S.T., Shindell, D.T., Skeie, R.B., Sudo, K., Szopa, S., Takemura, T., Zeng, G., 2012. Global air quality and climate. Chemical Society Review 41, 6663–6683.
Hansen, J., Sato, M., Ruedy, R., Nazarenko, L., Lacis, A., Schmidt, G.A., Russell, G., Aleinov, I., Bauer, M., Bauer, S., Bell, N., Cairns, B., Canuto, V., Chandler, M., Cheng, Y., Del Genio, A., Faluvegi, G., Fleming, E., Friend, A., Hall, T., Jackman, C., Kelley, M., Kiang, N., Koch, D., Lean, J., Lerner, J., Lo, K., Menon, S., Miller, R., Minnis, P., Novakov, T., Oinas, V., Perlwitz, J., Perlwitz, J., Rind, D., Romanou, A., Shindell, D., Stone, P., Sun, S., Tausnev, N., Thresher, D., Wielicki, B., Wong, T., Yao, M., Zhang, S., 2005. Efficacy of climate forcing. Journal of Geophysical Research 110, D18104. http://dx.doi.org/10.1029/2005JD005776.
Huijnen, V., Williams, J., van Weele, M., van Noije, T., Krol, M., Dentener, F., Segers, A., Houweling, S., Peters, W., de Laat, J., Boersma, F., Bergamaschi, P., van Velthoven, P., Le Sager, P., Eskes, H., Alkemade, F., Scheele, R., Nédélec, P., Pätz, H.-W., 2010. The global chemistry transport model TM5: description and evaluation of the tropospheric chemistry version 3.0. Geoscientific Model Development 3, 445–473.
Kloster, S., Dentener, F., Feichter, J., Raes, F., van Aardenne, J., Roeckner, E., Lohmann, U., Stier, P., Swart, R., 2008. Influence of future air pollution mitigation strategies on total aerosol radiative forcing. Atmospheric Chemistry and Physics 8, 6405–6437.
Koornneef, J., Ramirez, A., van Harmelen, T., 2010. The impact of CO_2 capture in the power and heat sector on the emission of SO_2, NO_x, particulate matter, volatile organic compounds and NH_3 in the European Union. Atmospheric Environment 44, 1369–1385.
Lamarque, J.-F., Page Kyle, G., Meinshausen, M., 2011. Global and regional evolution of short-lived radiatively-active gases and aerosols in the Representative Concentration Pathways. Climatic Change 109, 191–212.
Lamarque, J.-F., Shindell, D.T., Josse, B., Young, P.J., Cionni, I., Eyring, V., Bergmann, D., Cameron-Smith, P., Collins, W.J., Doherty, R., Dalsoren, S., Faluvegi, G., Folberth, G., Ghan, S.J., Horowitz, L.W., Lee, Y.H., MacKenzie, I.A., Nagashima, T., Naik, V., Plummer, D., Righi, M., Rumbold, S.T., Schulz, M., Skeie, R.B., Stevenson, D.S., Strode, S., Sudo, K., Szopa, S., Voulgarakis, A., Zeng, G., 2013. The Atmospheric Chemistry and Climate Model Intercomparison Project (ACCMIP): overview and description of models, simulations and climate diagnostics. Geoscientific Model Development 6, 179–206.
Lucas, P.L., van Vuuren, D.P., Olivier, J.G.J., den Elzen, M.G.J., 2007. Long-term reduction potential of non-CO_2 greenhouse gases. Environmental Science and Policy 10, 85–103.
Masui, T., Matsumoto, K., Hijoka, Y., Kinoshita, T., Nozawa, T., Ishiwatari, S., Kato, E., Shukla, P.R., Yamagata, Y., Kainuma, M., 2011. An emission pathway for stabilization at 6 W m^{-2} radiative forcing. Climatic Change 109, 59–76.
Meinshausen, M., Raper, S.C.B., Wigley, T.M.L., 2011a. Emulating coupled atmosphere-ocean and carbon cycle models with a simpler model, MAGICC6-Part 1: model description and calibration. Atmospheric Chemistry and Physics 11, 1417–1456.
Meinshausen, M., Smith, S.J., Calvin, K., Daniel, J.S., Kainuma, M.L.T., Lamarque, J.-F., Matsumoto, K., Montzka, S.A., Raper, S.C.B., Riahi, K., Thomson, A., Velders, G.J.M., van Vuuren, D.P., 2011b. The RCP greenhouse gas concentrations and their extensions from 1765 to 2300. Climatic Change 109, 213–241.
Moss, R.H., Edmonds, J.A., Hibbard, K.A., Manning, M.R., Rose, S.K., van Vuuren, D.P., Carter, T.R., Emori, S., Kainuma, M., Kram, T., Meehl, G.A., Mitchell, J.F.B., Nakicenovic, N., Riahi, K., Smith, S.J., Stouffer, R.J., Thomson, A.M., Weyant, J.P., Wilbanks, T.J., 2010. The next generation of scenarios for climate change research and assessment. Nature 463, 747–756.
Myhre, G., Samset, B.H., Schulz, M., Balkanski, Y., Bauer, S., Berntsen, T.K., Bian, H., Bellouin, N., Chin, M., Diehl, T., Easter, R.C., Feichter, J., Ghan, S.J., Hauglustaine, D., Iversen, T., Kinne, S., Kirkevåg, A., Lamarque, J.-F., Lin, G., Liu, X., Lund, M.T., Luo, G., Ma, X., van Noije, T., Penner, J.E., Rasch, P.J., Ruiz, A., Seland, Ø., Skeie, R.B., Stier, P., Takemura, T., Tsigaridis, K., Wang, P., Wang, Z., Xu, L., Yu, H., Yu, F., Yoon, J.-H., Zhang, K., Zhang, H., Zhou, C., 2013. Radiative forcing of the direct aerosol effect from AeroCom phase II simulations. Atmospheric Chemistry and Physics 13, 1853–1877.
Nakićenović, N., Alcamo, J., Davis, G., de Vries, B., Fenhann, J., Gaffin, S., Gregory, K., Griibler, A., Jung, T.Y., Kram, T., Lebre La Rovere, E., Michaelis, L., Mori, S., Morita, T., Pepper, W., Pitcher, H., Price, L., Riahi, K., Roehrl, A., Rogner, H.-H., Sankovski, A., Schlesinger, M., Shukla, P., Smith, S., Swart, R., van Rooijen, S., Victor, N., Dadi, Z., 2000. Special Report on Emissions Scenarios. A Special Report of Working Group III of the Intergovernmental Panel on Climate Change. Cambridge University Press, Cambridge, United Kingdom and New York, NY, USA, p. 599.
OECD, 2012. OECD Environmental Outlook to 2050. OECD Publishing. http://dx.doi.org/10.1787/9789264122246-en.
Pozzer, A., Zimmermann, P., Doering, U.M., van Aardenne, J., Tost, H., Dentener, F., Janssens-Maenhout, G., Lelieveld, J., 2012. Effects of business-as-usual anthropogenic emissions on air quality. Atmospheric Chemistry and Physics 12, 6915–6937.
Prather, M.J., Gauss, M., Berntsen, T., Isaksen, I., Sundet, J., Bey, I., Brasseur, G., Dentener, F., Derwent, R., Stevenson, D., Grenfell, L., Hauglustaine, D., Horowitz, L., Jacob, D., Mickley, L., Lawrence, M., Von Kuhlmann, R., Muller, J.-F., Pitari, G., Rogers, H., Johnson, M., Pyle, J., Law, K., van Weele, M., Wild, O., 2003. Fresh air in the 21st century. Geophysical Research Letters 30, 1100. http://dx.doi.org/10.1029/2002GL016285.
Prather, M.J., Holmes, C.D., Hsu, J., 2012. Reactive greenhouse gas scenarios: systematic exploration of uncertainties and the role of atmospheric chemistry. Geophysical Research Letters 39, L09803. http://dx.doi.org/10.1029/2012GL051440.
Riahi, K., Rao, S., Krey, V., Cho, C., Chirkov, V., Fischer, G., Kindermann, G., Nakicenovic, N., Rafaj, P., 2011. RCP-8.5: exploring the consequence of high emission trajectories. Climatic Change 109, 33–57.
Shindell, D., Kuylenstierna, J.C.I., Vignati, E., Van Dingenen, R., Amann, M., Klimont, Z., Anenberg, S.C., Muller, N., Janssens-Maenhout, G., Raes, F., Schwartz, J., Faluvegi, G., Pozzoli, L., Kupiainen, K., Höglund-Isaksson, L., Emberson, L., Streets, D., Ramanathan, V., Hicks, K., Oanh, N.T.K., Milly, G., Williams, M., Demkine, V., Fowler, D., 2012. Simultaneously mitigating near-term climate change and improving human health and food security. Science 335, 183–189.
Stevenson, D.S., Dentener, F.J., Schultz, M.G., Ellingsen, K., van Noije, T.P.C., Wild, O., Zeng, G., Amann, M., Atherton, C.S., Bell, N., Bergmann, D.J., Bey, I., Butler, T., Cofala, J., Collins, W.J., Derwent, R.G., Doherty, R.M., Drevet, J., Eskes, H.J., Fiore, A.M., Gauss, M., Hauglustaine, D.A., Horowitz, L.W., Isaksen, I.S.A., Krol, M.C., Lamarque, J.-F., Lawrence, M.G., Montanaro, V., Müller, J.-F., Pitari, G., Prather, M.J., Pyle, J.A., Rast, S., Rodriguez, J.M., Sanderson, M.G., Savage, N.H., Shindell, D.T., Strahan, S.E., Sudo, K., Szopa, S., 2006. Multimodel ensemble simulations of present-day and near-future tropospheric ozone. Journal of Geophysical Research 111, D08301. http://dx.doi.org/10.1029/2005JD006338.
Stevenson, D.S., Young, P.J., Naik, V., Lamarque, J.-F., Shindell, D.T., Voulgarakis, A., Skeie, R.B., Dalsoren, S.B., Myhre, G., Berntsen, T.K., Folberth, G.A., Rumbold, S.T., Collins, W.J., MacKenzie, I.A., Doherty, R.M., Zeng, G., van Noije, T.P.C., Strunk, A., Bergmann, D., Cameron-Smith, P., Plummer, D.A., Strode, S.A., Horowitz, L., Lee, Y.H., Szopa, S., Sudo, K., Nagashima, T., Josse, B., Cionni, I., Righi, M., Eyring, V., Conley, A., Bowman, K.W., Wild, O., Archibald, A., 2013. Tropospheric ozone changes, radiative forcing and attribution to emissions in the Atmospheric Chemistry and Climate Model Intercomparison Project (ACCMIP). Atmospheric Chemistry and Physics 13, 3063–3085.
Taylor, K.E., Stouffer, R.J., Meehl, G.A., 2012. An overview of CMIP5 and the experiment design. Bulletin of the American Meteorological Society 93, 485–498.
Thomson, A.M., Calvin, K.V., Smith, S.J., Kyle, G.P., Volke, A., Patel, P., Delgado-Arias, S., Bond-Lamberty, B., Wise, M.A., Clarke, L.E., Edmonds, J.A., 2011. RCP4.5: a pathway for stabilization of radiative forcing by 2100. Climatic Change 109, 77–94.
Van Aardenne, J., Dentener, F., Van Dingenen, R., Maenhout, G., Marmer, E., Vignati, E., Russ, P., Szabo, L., 2010. Climate and Air Quality Impacts of Combined Climate Change and Air Pollution Policy Scenarios. Joint Research Centre Scientific and Technical Research Reports, EUR 24572 EN, p. 71.
Van Vuuren, D.P., den Elzen, M.G.J., Lucas, P.L., Eickhout, B., Strengers, B.J., van Ruijven, B., Wonink, S., van Houdt, R., 2007. Stabilizing greenhouse gas concentrations at low levels: an assessment of reduction strategies and costs. Climatic Change 81, 119–159.
Van Vuuren, D.P., Meinshausen, M., Plattner, G.-K., Joos, F., Strassmann, K.M., Smith, S.J., Wigley, T.M.L., Raper, S.C.B., Riahi, K., de la Chesnaye, F., den Elzen, M.G.J., Fujino, J., Jiang, K., Nakicenovic, N., Paltsev, S., Reilly, J.M., 2008. Temperature increase in the 21st century mitigation scenarios. Proceedings of the National Academy of Sciences of the United States of America 105, 15258–15262.
Van Vuuren, D.P., Edmonds, J., Kainuma, M., 2011a. The Representative Concentration Pathways: an overview. Climatic Change 109, 5–31.
Van Vuuren, D.P., Stehfest, E., den Elzen, M.G.J., Kram, T., van Vliet, J., Deetman, S., Isaac, M., Klein Goldewijk, K., Hof, A., Beltran, A.M., Oostenrijk, R., van Ruijven, B., 2011b. RCP2.6: exploring the possibility to keep global mean temperature change below 2 degree C. Climatic Change 109, 95–116.
Van Vuuren, D.P., Bouwman, L.F., Smith, S.J., Dentener, F., 2011c. Global projections for anthropogenic reactive nitrogen emissions to the atmosphere: an assessment of scenarios in the scientific literature. Current Opinion in Environmental Sustainability 3, 359–369.

Wild, O., Fiore, A.M., Shindell, D.T., Doherty, R.M., Collins, W.J., Dentener, F.J., Schultz, M.G., Gong, S., MacKenzie, I.A., Zeng, G., Hess, P., Duncan, B.N., Bergmann, D.J., Szopa, S., Jonson, J.E., Keating, T.J., Zuber, A., 2012. Modelling future changes in surface ozone: a parameterized approach. Atmospheric Chemistry and Physics 12, 2037–2054.

Young, P.J., Archibald, A.T., Bowman, K.W., Lamarque, J.-F., Naik, V., Stevenson, D.S., Tilmes, S., Voulgarakis, A., Wild, O., Bergmann, D., Cameron-Smith, P., Cionni, I., Collins, W.J., Dalsøren, S.B., Doherty, R.M., Eyring, V., Faluvegi, G., Horowitz, L.W., Josse, B., Lee, Y.H., MacKenzie, I.A., Nagashima, T., Plummer, D.A., Righi, M., Rumbold, S.T., Skeie, R.B., Shindell, D.T., Strode, S.A., Sudo, K., Szopa, S., Zeng, G., 2013. Pre-industrial to end 21st century projections of tropospheric ozone from the Atmospheric Chemistry and Climate Model Intercomparison Project (ACCMIP). Atmospheric Chemistry and Physics 13, 2063–2090.